10.1515/astro-2017-0217

Baltic Astronomy, vol. 24, 176–184, 2015

ON EQUILIBRIUM FIGURES OF PARTICLE CLOUDS AROUND THE SUN AND STARS

B. P. Kondratyev[1,2] and N. G. Trubitsina[3]

[1] *Sternberg Astronomical Institute, M.V. Lomonosov Moscow State University, Universitetskij prospect 13, Moscow 119992, Russia*

[2] *The Central Astronomical Observatory of the Russian Academy of Sciences at Pulkovo, St. Petersburg; work@boris-kondratyev.ru*

[3] *Udmurt State university, Izhevsk, Russia*

Received: 2015 March 25; accepted: 2015 April 20

Abstract. Equilibrium figures of cold gas-dust (or cometary) clouds are studied in a more general setting than the classical Roche problem. The cloud is considered to be under the influence of gravitational attraction of the central star and the tidal field of the Galaxy. Our analysis also takes into account the centrifugal forces due to the rotation of the cloud, which moves around the center of the stellar system together with the star. The limit equilibrium figure is found to have three planes of symmetry and to be shaped like a "lemon" with lateral swellings and two singular points. The shape of this figure and its cusp angles in the planes of two main sections are calculated. The average density inside the equilibrium figure is shown to be almost exactly equal to the average density of matter in the Galaxy. This coincidence cannot be accidental and means that equilibrium figures with the critical level of the total surface potential fill the entire volume of the Galaxy. A possible consequence is that the cometary clouds of neighboring stars in the Galaxy may touch each other (or even intersect because of the presence of dark matter). Hence stars may exchange comets and part of the comets in the Solar System may belong to other stars.

Key words: celestial mechanics – Galaxy: solar neighborhood

1. INTRODUCTION

The study of the equilibrium and evolution of cold dense gas–dust clouds located in the vicinity of the Sun and other stars in the Galaxy is a problem of current interest. Such condensations are believed to consist of small-mass particles moving mainly under the influence of the gravitational field of the central star and significant perturbations due to the gravitational field of the Galaxy. The Oort cometary cloud is an example of such a condensation in the Solar System (see, e.g., Emelyanenko et al. 2007). Moreover, according to Hills (1981), there is a second massive cometary cloud surrounding the Sun.

The study of such clouds is a difficult problem, which has attracted the attention of many researchers, however, the available analyzes cannot be considered adequate from the point of view of the theory equilibrium figures. There are sev-

eral reasons for this. First, studying heterogeneous equilibrium figures is a rather challenging mathematical task (Kondratyev 1989). Second, such clouds around other stars are difficult to observe. However, there is now strong evidence for the existence of relic near-stellar clouds of particles. First of all, many astronomers agree that in the Solar System there is the huge Oort cometary cloud. Observations reveal such clouds around some other stars too (see, e.g., Nielsen at al. 2005). The discovery of many exoplanets in recent years also suggests that other stars may be surrounded by condensations of smaller particles. This is consistent with cosmogonical findings (Safronov 1969).

There are two approaches to the study of the dynamics of residual cold dust clouds. The first one is based on the analysis of orbits of small bodies in the gravitational field of the central star and in the combined field of the star and Galaxy (in the Solar System this is the case for the motions of comets in the Oort cloud). This problem was addressed by many authors, e.g., Breiter et al. (2008), Antonov & Baranov (2009). A number of other problems were analyzed by Rastorguev & Surdin (1978) and Ernst & Just (2013).

An alternative approach is to study the equilibrium states of compact clouds subjected to rotation and external gravitational fields. A classic example is a single lenticular Roche figure characterized by rigid rotation and extremely strong mass concentration to the center. This figure was studied by Roche (1879) and Jeans (1928). Actually, there is an entire series of equilibrium figures with the potential at the surface exceeding a certain critical value (see the book by Subbotin (1949) for some comments concerning this topic). Such figures are similar to gas equilibrium figures with the polytropic index $n = 5$ (see, e.g., Caimmi 1980). Kondratyev & Trubitsina (2013) developed an independent method for the analysis of a family of equilibrium figures.

King (2002) made some remarks concerning the shape of the Jacobi-integral surface, however, he did not analyze the shapes of equilibrium figures (see, also, Ossipkov 2006).

In this paper we investigate the equilibrium figures of cold gas–dust clouds in a more general context than that of the classical Roche problem. In the classical problem, the only source of force is the gravitating center, whereas our analysis takes into account the influence of the gravitational fields of both the central star and the Galaxy as well as the centrifugal forces due to the rotation of the cloud with the central star about the center of the stellar system. We investigate the properties of the equilibrium figure and some cosmogonical implications.

2. FORMULATION OF THE PROBLEM. THE TOTAL POTENTIAL

We assume that the Galaxy is an axisymmetric stellar system and introduce the cylindrical coordinates $R = \sqrt{x_1^2 + x_2^2}$ and x_3. The gravitational potential of the Galaxy $\Phi(R, x_3)$ includes the contribution of both baryonic and dark matter. We set the coordinates of the Sun or a star equal to $R = R_0$ and $x_3 = 0$, where R_0 is the distance to the Galactic Center.

We further assume that the test star (e.g., the Sun) is surrounded by a particle cloud. The center of mass of the cloud is located in the principal plane of the galaxy at a distance $R = R_0$ from its center and orbits around the center of the stellar system at an angular velocity of $\Omega\,(R, x_3)$. It follows from the balance of

the Galactic gravitational and centrifugal forces (Kondratyev 2003) that

$$\frac{\partial\Phi}{\partial R} = -\Omega^2 R_0\,; \quad \frac{\partial^2\Phi}{\partial R_0^2} = -\left(\Omega^2\left(R_0\right) + R_0\frac{d\Omega^2}{dR_0}\right). \tag{1}$$

We introduce the Cartesian coordinate system $O'x_1x_2x_3$ associated with the center of the cloud. The $O'x_1$ axis points in the direction of the Galactic center and the $O'x_2$ axis lies in the midplane of the Galaxy and points in the direction of the motion of the cloud around the center of the stellar system.

Each particle is subjected, in addition to the potential of the Galaxy, $\Phi(R, x_3)$, to the potential $\varphi\left(r\right)$ of the central star

$$\varphi\left(r\right) = \frac{Gm}{r}\,, \quad r = \sqrt{x_1^2 + x_2^2 + x_3^2}\,. \tag{2}$$

Because of the small size of the cloud compared to that of the Galaxy the particle coordinates R can be written as

$$R = \sqrt{\left(R_0 + x_1\right)^2 + x_2^2} \approx R_0 + x_1 + \frac{x_2^2}{2R_0}\,, \tag{3}$$

and the potential $\Phi(R, x_3)$ can be written in the tidal approximation

$$\Phi \approx \Phi_0 + \left(\frac{\partial\Phi}{\partial R}\right)_0 \cdot \left(R - R_0\right) + \\ + \frac{1}{2}\left(\frac{\partial^2\Phi}{\partial R^2}\right)_0 \cdot \left(R - R_0\right)^2 + \frac{1}{2}\left(\frac{\partial^2\Phi}{\partial x_3^2}\right)_0 \cdot x_3^2\,. \tag{4}$$

Given Eqs. (1) and (2), Galactic potential (4) acquires the form

$$\Phi \approx \Phi_0 - \Omega^2 R_0 \cdot \left(x_1 + \frac{x_2^2}{2R_0}\right) - \\ - \frac{1}{2}\left(\Omega^2 + R\frac{\partial\Omega^2}{\partial R}\right)_0 \cdot x_1^2 + \frac{1}{2}\left(\frac{\partial^2\Phi}{\partial x_3^2}\right)_0 \cdot x_3^2\,. \tag{5}$$

In addition, in the rotating coordinate system a particle is subjected to centrifugal force with the potential

$$\Phi_{\rm c} = \frac{1}{2}\left[\left(R_0 + x_1\right)^2 + x_2^2\right]\Omega^2\left(R_0\right). \tag{6}$$

We now combine Eqs. (3), (5), and (6) to obtain, after transformations and reductions of some terms, the following formula for the total potential $W\left(x_1, x_2, x_3\right)$ of the forces acting on the particle cloud:

$$W = \frac{Gm}{r} - \frac{1}{2}R\frac{d\Omega^2}{dR}\cdot x_1^2 + \frac{1}{2}\frac{\partial^2\Phi}{\partial x_3^2}\cdot x_3^2\,. \tag{7}$$

In formula (7) we drop the now unnecessary subscript "0". Given that potential is always determined up to a constant, we also drop the terms Φ_0 and $\frac{1}{2}R_0^2\Omega^2$. Note that the last two terms in potential (7) are quadratic functions of Cartesian coordinates.

With Oort's constants (see, e.g., Chandrasekhar 2005 and Ogorodnikov 1958)

$$A = \frac{1}{2}\left(\Omega - \frac{\partial v_\theta}{\partial R}\right); \quad B = -\frac{1}{2}\left(\Omega + \frac{\partial v_\theta}{\partial R}\right), \tag{8}$$

the first coefficient in the right-hand part of Eq. (7) can be written as

$$-\frac{1}{2}R\frac{d\Omega^2}{dR} = 2A\,(A - B) = K_1\,. \tag{9}$$

The second coefficient in Eq. (7) is

$$\frac{\partial^2\Phi}{\partial x_3^2} = -2K_3\,. \tag{10}$$

Note that for standard galaxy models with matter concentrated toward the symmetry plane the coefficient K_3 is always positive:

$$K_3 > 0\,. \tag{11}$$

The situation is not so straightforward for the coefficient K_1 where we have several options. In standard galaxies, where function $\Omega\,(R)$ decreases from the center toward the periphery, $K_1 > 0$. If the star resides in a rigid-rotation zone, $K_1 = 0$. If the star is located in a zone of abnormal rotation, e.g., in a region of a sharp minimum of rotational speed (Kondratyev 2014), the coefficient K_1 reverses its sign. In the solar neighborhood the standard inequality is evidently fulfilled:

$$K_1 > 0\,. \tag{12}$$

Thus, in our case the total potential is

$$W = \frac{Gm}{r} + K_1 \cdot x_1^2 - K_3 \cdot x_3^2\,. \tag{13}$$

Note that, since the total gravity force should be perpendicular to the $W = \text{const}$ surface, one of the surfaces should coincide with the boundary of the equilibrium figure. Let us study the shape of this figure.

3. LIMIT EQUILIBRIUM FIGURE WITH THE CRITICAL POTENTIAL

First, since r is small near the coordinate origin, the term Gm/r in Eq. (13) outweighs all the other terms; in this case, potential W takes on high values and the $W = \text{const}$ surfaces are closed and almost spherical. At a large distance from the center, potential W is small and the equipotential surfaces $W = \text{const}$ become opened and their meridional sections resemble hyperboles. Hence there should be such critical potential W^* that separates closed and open equipotential surfaces $W = \text{const}$. To find the critical W^* potential, we solve the following equation:

$$\frac{\partial W}{\partial x_1} = 0, \quad x_2 = x_3 = 0\,. \tag{14}$$

It yields the limit value x_1^*:

$$x_1^* = \left(\frac{Gm}{2K_1}\right)^{\frac{1}{3}}, \tag{15}$$

which determines the extent of the equilibrium figure along the Ox_1 axis. We now substitute the values $x_2 = x_3 = 0$ and x_1^* from Eq. (15) into Eq. (13) to find the required critical potential W^*:

$$W^* = \frac{3}{2}(Gm)^{\frac{2}{3}}(2K_1)^{\frac{1}{3}}. \tag{16}$$

Recall that the equipotential figures with $W \geq W^*$ are closed, and this is the case that will interest us further.

After the normalization of the coordinates equation (13), the limit figure acquires the form

$$3 = \frac{2}{\sqrt{x_1^2 + x_2^2 + x_3^2}} + x_1^2 - kx_3^2, \quad k = \frac{K_3}{K_1}. \tag{17}$$

We now investigate equation (17).

To this end, we find the main cross sections of the limit figure: the cross section in the Ox_1x_3 plane

$$3 = \frac{2}{\sqrt{x_1^2 + x_3^2}} + x_1^2 - kx_3^2 \tag{18}$$

shown in Fig. 1; the cross section in the Ox_2x_3 plane

$$3 = \frac{2}{\sqrt{x_2^2 + x_3^2}} - kx_3^2 \tag{19}$$

shown in Fig. 2; and the cross section in the Ox_1x_2 plane

$$3 = \frac{2}{\sqrt{x_1^2 + x_2^2}} + x_1^2 \tag{20}$$

shown in Fig. 3.

4. NUMERICAL CALCULATIONS

We now perform the calculations using known parameters based on observations of the solar neighborhood. According to Olling & Merrifield (1998), the Oort constants are equal to

$$A = 11.3 \text{ km s}^{-1} \text{ kpc}^{-1}; \quad B = -13.9 \text{ km s}^{-1} \text{ kpc}^{-1}. \tag{21}$$

Given Eq. (21) and the results of Kuijken & Gilmore (1989), the coefficients in formula (13) are equal to

$$K_1 = 569.52 \text{ km}^2 \text{ s}^{-2} \text{ kpc}^{-2} = 0.598 \cdot 10^{-30} \text{s}^{-2};$$

$$K_3 = 392.5 \text{ km}^2 \text{ s}^{-2} \text{ kpc}^{-2} = 0.412 \cdot 10^{-30} \text{s}^{-2}; \tag{22}$$

$$k = 0.36275.$$

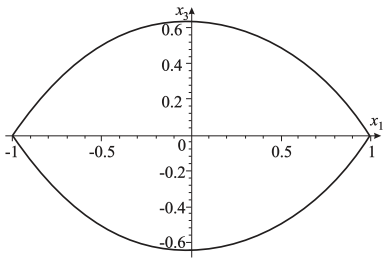

Fig. 1. Cross section of the figure in the Ox_1x_3 plane.

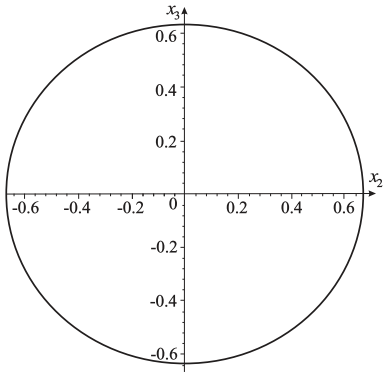

Fig. 2. Cross section of the figure in the Ox_2x_3 plane. Here $-2/3 \le x_2/x_1^* \le 2/3$, and x_3 is the root of the cubic equation $3 = 2x_3^{-1} - kx_3^2$, which is equal to ≈ 0.6356. This curve resembles an ellipse with a small oblateness ($\varepsilon \approx 0.0466$).

The 3D equilibrium figure is shown in Fig. 4. It has three planes of symmetry and its shape is similar to a "lemon" with lateral swellings and only two singular points.

Note that the lateral swellings of this figure represent the conical points. To find the cusp angles in the main Ox_1x_3 plane, it is necessary to calculate the derivative of the implicit function $F(x_1, x_3)$ defined by formula (18):

$$\frac{dx_1}{dx_3} = -\frac{\frac{\partial F}{\partial x_1}}{\frac{\partial F}{\partial x_3}} = -\frac{x_1}{x_3}\frac{1 - \left(x_1^2 + x_3^2\right)^{\frac{3}{2}}}{1 + k(x_1^2 + x_3^2)^{\frac{3}{2}}}. \tag{23}$$

However, at the cusp point ($x_3 = 0, x_1 = 1$), formula (23) has an indeterminacy of the $\frac{0}{0}$ form. We evaluate this uncertainty to obtain, after cumbersome manipulations (which we omit here) and the important non-trivial remark that should take the square root of the result, the following half wedge angle in the Ox_1x_3 plane:

$$\tan\theta_{13} = \sqrt{\frac{3}{1+k}}. \tag{24}$$

However, as we already know, in the solar neighborhood $k = 0.36275$, and hence the total wedge angle of the figure in the Ox_1x_3 plane is equal to

$$2\theta_{13} = 112.04^\circ. \tag{25}$$

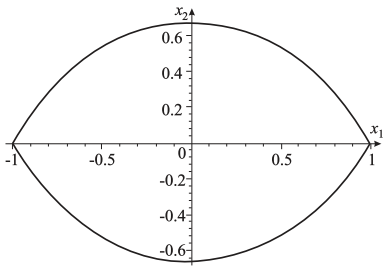

Fig. 3. Cross section of the figure in the Ox_1x_2 plane.

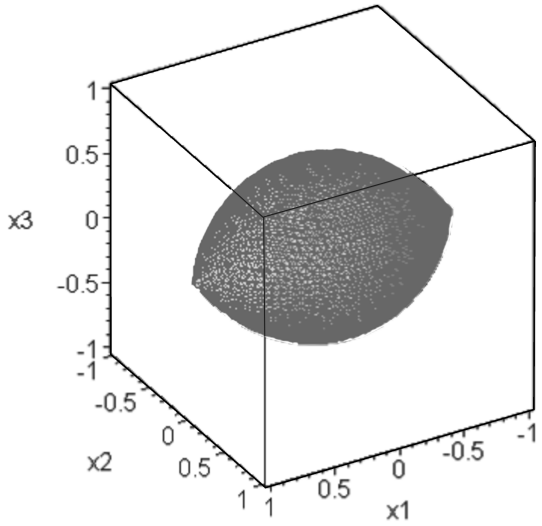

Fig. 4. 3D-image of the limit equilibrium figure in the vicinity of the Sun. The figure has two special points – these are the end points along the $O'x_1$ axis directed radially from the Galactic center.

This angle differs markedly from the $2\theta_{13} = 120^\circ$ cusp angle of the classical Roche equilibrium figure.

We similarly find the wedge angle of the figure in the Ox_1x_2 plane, which is more obtuse:

$$2\theta_{12} = 120^\circ. \tag{26}$$

The cross section in the Ox_2x_3 plane resembles an ellipse with a small oblateness ($\varepsilon \approx 0.0466$).

Thus, whereas in the case of the classical lenticular Roche figure the singular points fill the entire equator, our limit figure has only two singular points.

5. DISCUSSION AND COSMOGONIC IMPLICATIONS

Above, we found that the equilibrium figure of the particle cloud in Fig. 4 has three planes of symmetry and only two singular points. The shape of this figure differs markedly from that of the Roche figure. An analysis of the properties of

the equilibrium figure is of great interest, and now we want to draw attention to the following fact.

Calculations show that the volume of the "lemon" in Fig. 4 is approximately equal to

$$V \approx 0.565\,\pi\, {x_1^*}^3. \tag{27}$$

Hence the average density of matter $\tilde{\rho} = m/V$ inside the figure is

$$\tilde{\rho} = \frac{2K_1}{0.565\pi G} \approx 1.014 \cdot 10^{-23}\,\mathrm{g\,cm^{-3}}. \tag{28}$$

On the other hand, according to the upper estimate of the density in the Galactic midplane (see, e.g., King 2002), the average density of matter in the Galaxy is

$$\rho_0 = 0.15\,M_\odot\,\mathrm{pc}^{-3}, \quad \text{or} \quad \rho_0 \approx 1.027 \cdot 10^{-23}\,\mathrm{g\,cm^{-3}}. \tag{29}$$

A comparison of the density estimates (29) and (28) leads us to an interesting conclusion: these two densities are closely equal and hence the entire volume of the Galaxy should be completely filled by the equilibrium figures considered here with the surface potential equal to the critical value of $W^* = \frac{3}{2}(Gm)^{\frac{2}{3}}(2K_1)^{\frac{1}{3}}$. This figure appears to be the unit cell of the 3D structure of the Galaxy. Such a remarkable coincidence cannot be accidental. A possible implication is that the cometary clouds of neighboring stars in the Galaxy should touch each other. Moreover, given that that the average density of matter in the Galaxy slightly exceeds the average density of matter in these equilibrium figures (especially if we take into account the presence of dark matter), these critical surfaces should even intersect each other.

Indeed, according to the formula (15), the half diameter of the figures is equal to

$$x_1^* \approx 1.5\,\mathrm{pc}\,. \tag{30}$$

Hence stars can exchange their comets, some of the comets in the Solar System may originate from other stars. This result expands our views on the nature of comets. This is, however, unlikely to be the case for retrograde comets, because they are confined by Coriolis force.

REFERENCES

Antonov V. A., Baranov A. S. 2009, Astrophysica, 52, 435
Breiter S., Fouchard M., Ratajczak R. 2008, MNRAS, 383, 200
Caimmi R. 1980, Ap&SS, 71, 415
Chandrasekhar S. 2005, *Principles of Stellar Dynamics*, Dover, New York
Emelyanenko V. V., Asher D.J., Bailey M. E. 2007, MNRAS, 381, 779
Ernst A., Just A. 2013, MNRAS, 429, 2953
Hills J. G. 1981, Astron. J., 86, 1730
Jeans J. H. 1928, *Astronomy and Cosmogony*, Cambridge Univ. Press, Cambridge
King A. R. 2002, *Introduction to Classical Stellar Dynamics* (In Russian, Translated from English), Editorial URSS, Moscow
Kondratyev B. P. 1989, *Dynamics of Gravitating Ellipsoidal Figures*, Nauka, Moscow
Kondratyev B. P. 2003, *The Potential Theory and Equilibrium Figures*, RHD, Moscow-Izhevsk

Kondratyev B. P. 2014, MNRAS, 442, 1755
Kondratyev B. P., Trubitsina N. G. 2013, Astron. Nachr., 334, 879
Kuijken K., Gilmore G. 1989, MNRAS, 239, 605
Nielsen K. E., Gull T. R., Vieira Kober G. 2005, ApJS, 157, 138
Ogorodnikov K. F. 1958, *Dynamics of Stellar Systems*, Fizmatgiz, Moscow
Olling R. P., Merrifield M. R. 1998, MNRAS, 297, 943
Ossipkov L. P. 2006, Astron. Reports, 50, 116
Rastorguev S. A., Surdin V. G. 1978, Astron. Circ., 1016, 3
Roche E. 1879, *Essai sur la Constitution et l'Origine du Système solaire*, Mèm. Acad. Sci. de Montpellier, Section Sciences, vol. VIII
Safronov V. S. 1969, *Evolution of Protoplanetary Cloud and Formation of Earth and Planets*, Nauka, Moscow
Subbotin M. F. 1949, *Course of Celestial Mechanics*, GITTL, Moscow-Leningrad